THE JOURNAL OF PHYSICAL CHEMISTRY B

Article

pubs.acs.org/JPCB

Pulsed-Field Gradient NMR Measurements on Hydrogels from Phosphocholine

Jürgen Linders,[†] Christian Mayer,*[,†] Tomoko Sekine,[‡] and Heinz Hoffmann[§]

[†]University Duisburg-Essen, CeNIDE, Universitätsstrasse 2, 45141, Germany

[‡]Shiseido Research Center, 2-2-1 Hayabuchi, Tsuzuki-ku, Yokohama 224-8558, Japan

[§]University of Bayreuth, BZKG/BayColl, Gottlieb-Keim-Strasse 60, 95448 Bayreuth, Germany

Supporting Information

ABSTRACT: Gels from diacylphosphatidylcholine in glycerol/butylene glycol mixtures were investigated by pulsed-field gradient NMR measurements. Previous measurements had shown that the gels are formed by networks from crystalline multilamellar vesicles (MLV). The obtained self-diffusion coefficients for water and butylene glycol molecules indicate that both molecules occur in two different environments, even at temperatures above the phase transition T_m where the system is still in a liquid crystalline state. While the larger fraction of the molecules shows a free self-diffusion process like in a homogeneous phase, the smaller fraction seems to be encapsulated in closed domains and undergoes only hindered self-diffusion. It is concluded that the hindered diffusions are due to the solvent molecules trapped between the bilayers of the multilamellar vesicles, while the free diffusion is assigned to the solvent molecules outside of the MLV. Since the fraction of the entrapped molecules does not change during phase transition, we assume that the structure of the network in the samples remains the same when gelation occurs. The gelation process is simply due to the transformation of the vesicle bilayers from the liquid crystalline to the crystalline state. The permeability of the bilayer for the solvent molecules is drastically changed by this transition. The exchange of water molecules through the bilayers slows down significantly below T_m: while the average residence time of water molecules inside the vesicles is smaller than 50 ms in the liquid crystalline state, this value increases to more than 1 s for the gel state. In the case of pure butylene glycol, no vesicles are present, and it is likely that these gels are formed from crystalline fibers.

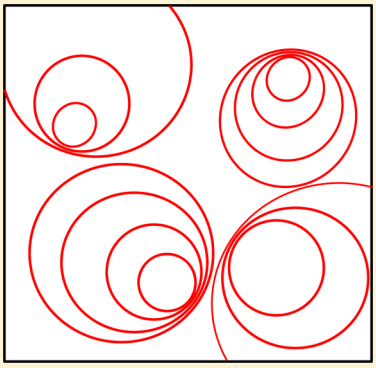

INTRODUCTION

In aqueous solutions, phosphocholine (PC) molecules form dispersions of small particles.[1−5] Above the melting temperature T_m of the PC, the bilayers can take up some water for the solvation of the PC head groups. The PC bilayers then are separated by thin aqueous bilayers of about the same thickness as the PC bilayers.[6] Dispersions of such phases can be transformed into vesicle phases by various procedures like extrusion processes,[7] sonication procedures[8] or dissolving the PC in solvents which are soluble in water and can be mixed with water.[9] Recently, it was shown that the bilayers in the L_α-phases swell to large separations of up to 100 nm when solvents are added to the aqueous solutions which do not change the hydrophobic interaction but increase the refractive index of the aqueous phase.[10] On matching the refractive index of the solvent with the refractive index of the bilayers, the particles of the L_α-phases swell to form single-phase transparent samples. The reason for the swelling is the decrease of the Hamaker constant for the attraction between the bilayers.[11] In the point of index matching, the attraction between the bilayers becomes so small that it can be overcome by the repulsive undulation forces. This behavior had been demonstrated with several cosolvents like glycerol, DMSO, polyhydroxy compounds like glucose, and L_α-phases from block-copolymers, surfactants, and lecithin. Recently, it was shown that such highly swollen L_α-phases from phosphocholine that contain only one to a few percent of PC gellify when the samples are cooled below the melting temperature T_m of the PC.[12]

The reason for the gelation process turned out to be the formation of a three-dimensional network of multilamellar vesicles (MLV) with thin bilayers in the crystalline state. Obviously, the crystalline bilayers are much stiffer than the bilayers in the liquid crystalline state and for that reason can no longer undulate.[13] The repulsive interaction between the bilayers therefore disappears, and the vesicles can form sticky contacts. Conductivity data on such phases in the presence of salt indicated that the conductivity decreased dramatically upon gelation. It was assumed that this decrease was mainly given by the loss of permeability of the bilayers for small ions. It was expected that the permeability of the bilayers would also change for water molecules and other small neutral molecules. Therefore, it should be possible to separate solvent molecules from inside and outside of the vesicles by pulsed-field gradient NMR measurements (PFG-NMR).[14−16] The following study is meant to elucidate the self-diffusion behavior of butylene glycol and water in different phase states of the system.

Received: May 14, 2012
Revised: August 27, 2012
Published: August 27, 2012

   dx.doi.org/10.1021/jp3046565 | J. Phys. Chem. B 2012, 116, 11459−11465

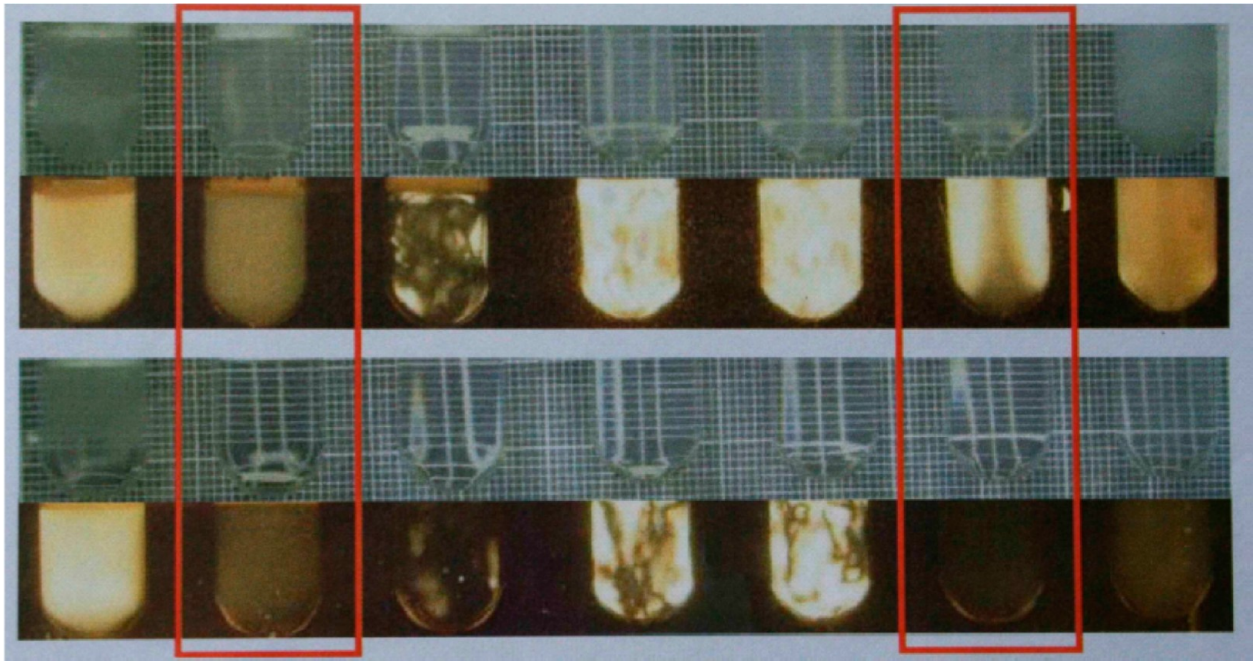

Figure 1. One percent PC samples in 1,3-butylene glycol/glycerol mixtures with the mixing ratios 0/10, 2/8, 4/6, 5/5, 6/4, 8/2, and 10/0 (from left to right), photographed directly and in between polarizers. The top two rows refer to the gel state at 25 °C, and the lower two rows refer to the liquid crystalline state at 60 °C. Note that the sample with pure butylene glycol (outermost right column) is optically isotropic at 60 °C but birefringent in the gel state.

EXPERIMENTAL SECTION

Cryo-TEM. The cryo-TEM micrographs were taken from a sample with 20% butylene glycol and 80% glycerol to which 4% of PC was added. After gelation, the gel was mechanically broken, and the destroyed sample was diluted with water by a factor of 3. The final sample thus contained about 1% PC.

PFG-NMR. For the preparation of the PFG-NMR samples, we start with a mixture of PC together with 1,3-butylene glycol and glycerol in the desired relation (10/0, 8/2, 6/4, 4/6, 2/8, and 0/10). Prior to the measurement, water is added to the mixture up to a final content of 33 wt %, and the sample is carefully homogenized at elevated temperature by slow gravitational flow. The resulting material is filled into a regular 3 mm NMR sample tube embedded in an outer 5 mm sample tube in order to minimize convection effects. Spacers are used to guarantee a defined inner tube position. Initial relaxation measurements have been performed in order to exclude the potential influence of spin−lattice and spin−spin relaxation to the echo decay profiles obtained in the PFG-NMR experiments (see Supporting Information).

All PFG-NMR-measurements are performed on a Bruker Avance 400 spectrometer (Bruker AG, Karlsruhe, Germany) equipped with a BAFPA 40 gradient amplifier and a Bruker DIFF30 probe. The instrument is tuned to 400 MHz proton frequency, and gradient pulses are adjusted to gradient strengths between 5 and 550 G/cm with individual durations of 2 ms. For all measurements, the stimulated echo ($90°$-τ_1-$90°$-τ_2-$90°$-τ_1-echo) is used in combination with the gradient pulses during each τ_1 waiting period. The duration of the $90°$ pulses is 9 μs, and the waiting period between the 96 repetitions (scans) of each experiment amounts to 5 s. The spacing Δ between the two gradient pulses is varied between 50 and 400 ms. The temperature of the sample is adjusted in a constant gas flow, and the absolute temperature setting in the probe is checked with a separate ethylene glycol sample.

The free induction decays resulting from the addition of each set of 96 experiments were Fourier transformed and analyzed for the echo signal decay vs the gradient strength G and the pulse spacing Δ. Characteristic signals were chosen for the individual observation of 1,3-butylene glycol and water. For the analysis of the diffusion profile, the relative signal intensities I/I_0 (I_0 referring to the signal intensity at gradient strength $G = 0$) are plotted logarithmically vs the parameter $\gamma^2G^2\delta^2(\Delta - \delta/3)$, with γ being the gyromagnetic ratio of protons, G the strength of the pulsed field gradient, and δ and Δ the duration of and the spacing between the two gradient pulses.

RESULTS

Figure 1 shows the seven samples that are investigated by the NMR measurements. The samples have the same solvent composition as the ones which have already been studied for their rheology and conductivity and by cryo-TEM.[12]

The samples contain 1% solutions of PC in the pure solvents glycerol (left column) and butylene glycol (right column) and solvent mixtures with BG/glycerol mixing ratios of 2/8, 4/6, 5/5, 6/4, 8/2 (in between, from left to right). The two lower rows show the samples at 60 °C, which is at a temperature above the melting temperature T_m of PC. The two upper rows show the samples at 25 °C, which is at a temperature below T_m, 55 °C. All samples were photographed directly and in between polarizers. All samples appear as more or less transparent single-phase liquids at 60 °C. At the same temperature, all samples with glycerol and the mixing ratio up to 6/4 have a strong stationary birefringence. Only the samples with a 8/2 mixing ratio and the solvent with pure butylene glycol show no birefringence and appear dark when observed between polarizers. When 10% of water was added to the 8/2 mixture, the liquid sample became also birefringent while the pure butylene glycol sample remained isotropic.[17]

dx.doi.org/10.1021/jp3046565 | J. Phys. Chem. B 2012, 116, 11459−11465

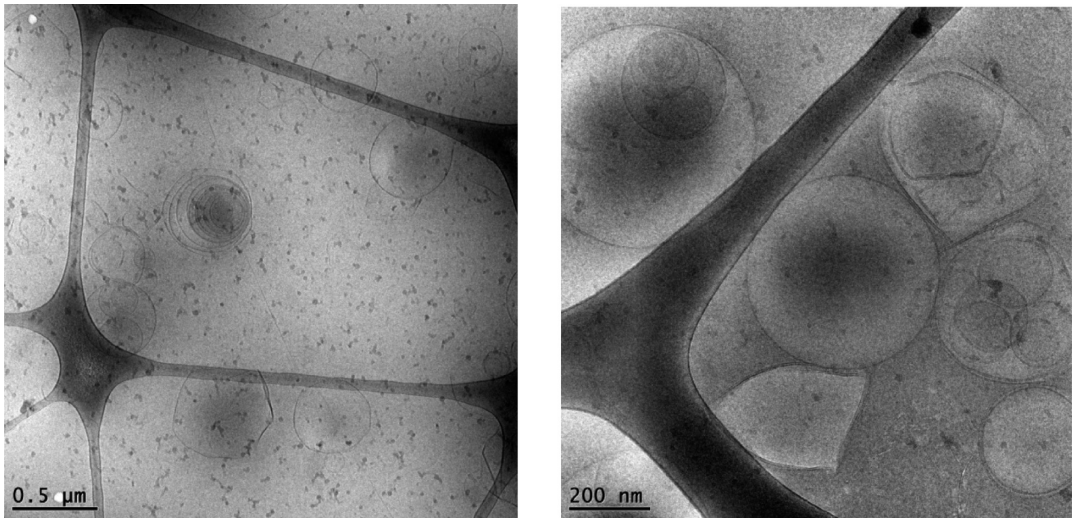

Figure 2. Cryo-TEM micrographs with 4% PC in 2/8 mixtures of butylene glycol and glycerol. After gelation, the samples were broken and diluted by a factor of 3 with water. Note that the bilayers in the MLV are in contact with each other.

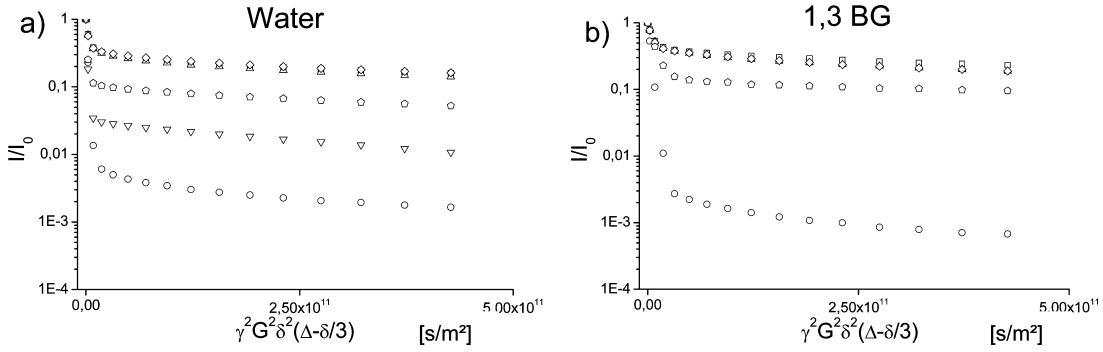

Figure 3. PFG-NMR echo decay plots for water (a) and 1,3-butylene glycol (b) of the L_α-phase at different relations B/G between 1,3-butylene glycol and glycerol at 332 K. The B/G relations are 10/0 (circles), 8/2 (squares), 6/4 (triangles), 4/6 (diamonds), and 2/8 (pentagons). At B/G = 0/10 (inverted triangles), only the water signal is detected. All plots are measured with a diffusion time of Δ = 50 ms. The extrapolation of the plateau values (last four data points have been used) to the I/I_0 axis reflects the relative contribution of those molecules which remain in the encapsulated volume over the given observation period of 50 ms.

In the gel state at 25 °C, the samples have turned into transparent gels which altogether are birefringent, including the sample in pure butylene glycol. The birefringence pattern in the liquid crystalline and in the gel state looks similar for each sample composition. However, a significant variation of the birefringence pattern between the samples of different compositions can be observed. The samples at 60 °C look like typical L_α-phases with multilamellar vesicles (MLV).[18] However, it was not possible to obtain good micrographs with the cryo-TEM method. The difficulty is due to the matching of the refractive index between the solvent and the bilayers: when the samples become transparent for visible light, the contrast of the PC structures also disappears for the electron beam.[19] However, in the gel state, the structures of the gel network can be broken and the fractured samples could be diluted with water. Under these conditions it was possible to obtain the micrographs shown in Figure 2.

In the TEM micrographs, one can still see large multi- and unilamellar vesicles with diameters of up to 1 μm. The large size of the vesicles is consistent with the observation that the samples in both the liquid and in the gelled state are birefringent. The enclosed vesicles in the MLV are not arranged with equal spacings between the bilayers. Instead, the bilayers touch each other at some defined locations. This is a consequence of the absence of the undulation process and a result of the attractive forces between the crystalline bilayers. The interlamellar distance between the bilayers is in the range of 50−100 nm. Some of the micrographs also show flat fragments which probably are the result of the mechanical destruction of the vesicles. It is also noteworthy that some vesicles are sitting on the grid of the polymer film. This is a sign that the bilayers of the vesicles are stiff and the vesicles do not collapse after the solvent has escaped.

The most remarkable feature of the micrographs is that the bilayers can clearly be seen as a double layer, that is, as the sum of two separate monolayers. This high resolution is probably a result of the crystalline state of the bilayers in which the local state of the individual molecules, in particular the orientation of their phosphate groups, is fixed. This is not the case in liquid crystalline bilayers in which the distance between the phosphate groups varies because of the thermal motion of the individual molecules.

All samples shown in Figure 1 have been subject to PFG-NMR measurements. The resulting echo decay plots on the L_α-phases (T = 332 K) of various compositions are shown in Figure 3. All measurements refer to a single diffusion time (gradient pulse spacing) of Δ = 50 ms and reflect the relative echo intensities I/I_0 for water (a) and 1,3-butylene glycol (b). In case of a free diffusion of the observed molecules, the graph of $\ln(I/I_0)$ vs the parameter $\gamma^2G^2\delta^2(\Delta - \delta/3)$ would result in a straight line with a

dx.doi.org/10.1021/jp3046565 | J. Phys. Chem. B 2012, 116, 11459−11465

slope identical to the negative self-diffusion constant. Hence, all plots in Figure 3 indicate the presence of two fractions of the observed molecules: a mobile one showing free diffusion (corresponding to the first, steep parts of the decay plots) and a more or less immobile, encapsulated one (corresponding to the second, flat parts of the decay plots). The level of the flat part of each decay plot on the I/I_0 scale marks the relative amount of those molecules which remain in the encapsulated state over the full observation period Δ. No significant differences are observed between the corresponding levels of water and 1,3-butylene glycol (a and b) for each sample.

In the absence of glycerol (relation between 1,3-butylene glycol and glycerol 10/0), the encapsulated fraction n_{cap} is very small. Estimated from the extrapolation of the flat part of the decay curve for Δ = 50 ms, it is represented by $n_{cap} \approx 0.002$. Hence, only about 0.2% of the observed molecules are in the encapsulated state. In the presence of glycerol, the fraction of encapsulated molecules rises dramatically. For the 1,3-butylene glycol/glycerol relations of 8/2, 6/4, and 4/6, the estimated values for n_{cap} are around 0.3, meaning that approximately 30% of the 1,3-butylene glycol and water molecules are encapsulated in small volumes such as vesicles. For higher glycerol concentrations, the value for n_{cap} is somewhat reduced: at a 1,3-butylene glycol/glycerol relation of 2/8, approximately 10% of the observed molecules are encapsulated, and for the relation 0/10 the value is further reduced to 2.5%. The resulting dependence between the encapsulated fraction and the 1,3-butylene glycol/glycerol relation is plotted in Figure 4.

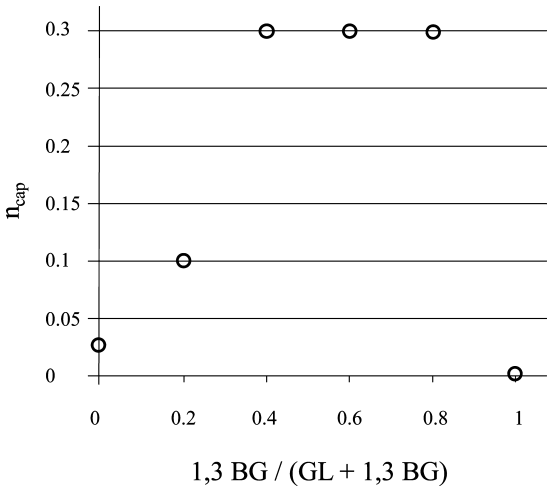

Figure 4. Relative contribution of the immobilized fractions of 1,3-butylene glycol and water (both values are identical within the error limits) as a function of the relation between 1,3-butylene glycol and glycerol. All values are estimations from the plateau levels of the decay curves in Figure 3; the points correspond to butylene glycol/glycerol relations of 0/10, 2/8, 4/6, 6/4, 8/2, and 10/0 (from left to right). The values refer to those molecules which remain in the encapsulated state for the period of 50 ms.

Figure 5 shows corresponding echo decay plots under variation of the diffusion time (gradient pulse spacing Δ) for 1,3-butylene glycol (left column) and water (right column). Again, all decay plots exhibit a steep part next to a flat one, indicating the presence of a mobile fraction next to a partially immobilized fraction. In addition, characteristic dependencies of the flat parts of the plots on the duration Δ are observed.

In the absence of glycerol (Figure 5a, b), the slope of the flat part strongly depends on Δ. For water as well as for 1,3-butylene glycol, the absolute slope for Δ = 400 ms is at least two times smaller than the one for Δ = 50 ms. That means that the apparent self-diffusion coefficient of the encapsulated fraction is larger for short observation times than for long ones, an observation which is typical for hindered self-diffusion. It is easily explained by assuming an encapsulation of the observed molecules in micrometer-sized volumes: at very short observation times, only few molecules come into contact with the diffusion barriers; hence, the observed diffusion pattern resembles the one for free diffusion. With an increasing observation period, the diffusing molecules experience more and more contacts with the barriers; hence, the apparent self-diffusion constant becomes smaller and smaller. On the other hand, with n_{cap} = 0.2%, the fraction of the encapsulated molecules is very small, as was derived from the discussion of Figure 3.

For medium glycerol contents (1,3-butylene glycol/glycerol relations of 8/2, 6/4, and 4/6), the effect of hindered diffusion is still detectable for the 1,3-butylene glycol: the final slopes of the echo decay curves slightly decrease with increasing diffusion times Δ (Figure 5c, e, and g). For water, on the other hand, the situation looks different (Figure 5d, f, and h). Here, the plateau values in the flat parts of the plots decrease with increasing Δ while the slopes roughly remain the same. This indicates a significant permeability of the diffusion barriers: with increasing observation time, less and less observed molecules remain in the encapsulated state, hereby leading to a decrease of the apparent encapsulated fraction with increasing Δ. The average residence time of water molecules can be estimated from a least-squares fit procedure on the set of decay curves.[26] For the plot in Figure 5f, a half-life time of 300 ±20 ms corresponding to an average residence time of 430 ±25 ms is found (see Supporting Information).

For the highest glycerol contents (1,3-butylene glycol/glycerol relations of 2/8 and 0/10), the rapid permeation is observed for both components, the 1,3-butylene glycol as well as water (Figure 5i, j, and k). In addition, all plots exhibit a significant dependence of the slope on the diffusion time Δ for the encapsulated fraction. Finally, a peculiar oscillation of $\ln(I/I_0)$ with increasing gradient strength can be observed which again is typical for a self-diffusion in a encapsulated phase.[20,21] In the case of the highest glycerol content (0/10), the set of decay plots for water in the L_α-phase is compared to the one obtained in the gel phase at 300 K (Figure 6). Below the phase transition, the plots for all diffusion times Δ are absolutely identical (Figure 6 a), an observation which is in strong contrast to the situation at higher temperature (Figure 6 b). Obviously, in the gel phase, all indications for a permeation of the compartments have disappeared. However, the relative contribution of the encapsulated molecules remains the same as is obvious from an extrapolation of the plateau values for both plots.

All diffusion constants deriving from the analysis of the echo decay curves in Figure 5 are listed in Table 1 (for water) and Table 2 (for 1,3-butylene glycol).

DISCUSSION

The optical appearances of the samples shown in Figure 1 clearly indicate that, even for a PC concentration of only 1%, all samples but the one in pure butylene glycol are single-phase liquid crystalline L_α-phases. At this small concentration of PC, the mean distance between the bilayers must be about 100 times larger than the thickness of a PC bilayer.

dx.doi.org/10.1021/jp3046565 | J. Phys. Chem. B 2012, 116, 11459−11465

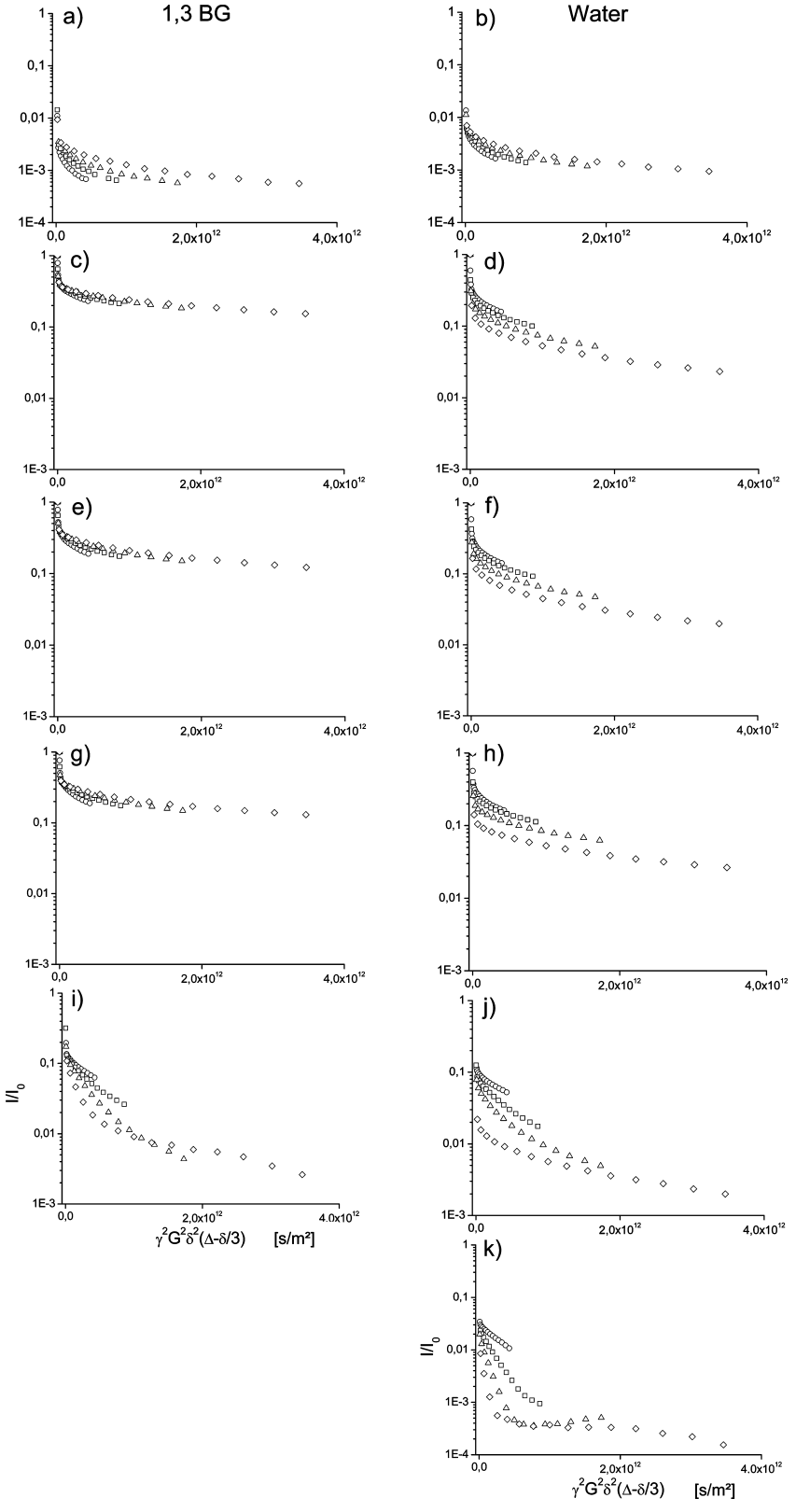

Figure 5. PFG-NMR echo decay plots for 1,3-butylene glycol (left column) and water (right column) of the L_α-phase at different relations between 1,3-butylene glycol and glycerol at 332 K. The B/G relations are 10/0 (a and b), 8/2 (c and d), 6/4 (e and f), 4/6 (g and h), and 2/8 (i and j). At $B/G = 0/10$ (k), only the water signal is detected. In all cases, the diffusion time Δ is varied between 50 and 400 ms (50 ms, circles; 100 ms, squares; 200 ms, triangles; 400 ms, diamonds).

In order to elucidate the mesoscopic structure behind this surprising constellation, nuclear magnetic resonance echo experiments with pulsed field gradients (PFG-NMR) have been carried out. This technique has proven to be a powerful approach for the analysis of heterogeneous systems.[22−25] The observation of the self-diffusion behavior of mobile components

dx.doi.org/10.1021/jp3046565 | J. Phys. Chem. B 2012, 116, 11459−11465

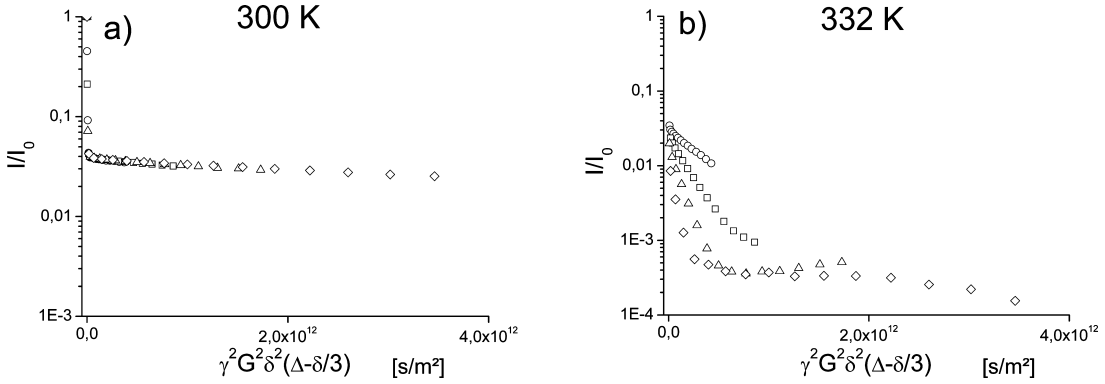

Figure 6. PFG-NMR echo decay plots for water in the gel phase (left) and in the L_α-phase (right) at a relation between 1,3-butylene glycol and glycerol of 0/10. In both cases, the diffusion time Δ is varied: 50 (circles), 100 (squares), 200 (triangles), and 400 ms (diamonds).

Table 1. Self Diffusion Constants of Water as Derived from the Echo Decay Plots in Figure 5 (Right Column)[a]

	self-diffusion constants for water (m^2/s)							
Δ	50 ms		100 ms		200 ms		400 ms	
B/*G* relations	$D_{(free)}$	$D_{(hindered)}$	$D_{(free)}$	$D_{(hindered)}$	$D_{(free)}$	$D_{(hindered)}$	$D_{(free)}$	$D_{(hindered)}$
10/0	2.37×10^{-10}	1.33×10^{-12}	2.18×10^{-10}	7.59×10^{-13}	1.35×10^{-10}	3.68×10^{-13}	6.35×10^{-11}	2.08×10^{-13}
8/2	1.05×10^{-10}	9.21×10^{-13}	6.44×10^{-11}	6.40×10^{-13}	4.04×10^{-11}	3.88×10^{-13}	2.55×10^{-11}	2.51×10^{-13}
6/4	5.60×10^{-11}	1.06×10^{-12}	3.18×10^{-11}	6.53×10^{-13}	1.94×10^{-11}	4.09×10^{-13}	1.20×10^{-11}	2.59×10^{-13}
4/6	5.27×10^{-11}	9.12×10^{-13}	3.02×10^{-11}	5.51×10^{-13}	1.84×10^{-11}	3.48×10^{-13}	1.19×10^{-11}	2.08×10^{-13}
2/8	1.03×10^{-10}	1.19×10^{-12}	5.20×10^{-11}	1.27×10^{-12}	2.93×10^{-11}	7.24×10^{-13}	2.10×10^{-11}	3.85×10^{-13}
0/10	1.70×10^{-10}	2.37×10^{-12}	8.91×10^{-11}	2.05×10^{-12}	4.66×10^{-11}	4.58×10^{-13}	3.49×10^{-11}	5.53×10^{-13}

[a]The values $D_{(free)}$ refer to the free bulk water and are derived from the initial steep slope (first four data points) of the decay plots. The values $D_{(hindered)}$ refer to the encapsulated fraction and are determined from the last four data points of the shallow parts of the plots.

Table 2. Self-Diffusion Constants of 1,3-Butylene Glycol as Derived from the Echo Decay Plots in Figure 5 (Left Column)[a]

	self-diffusion constants for 1,3-butylene glycol (m^2/s)							
Δ	50 ms		100 ms		200 ms		400 ms	
B/*G* relations	$D_{(free)}$	$D_{(hindered)}$	$D_{(free)}$	$D_{(hindered)}$	$D_{(free)}$	$D_{(hindered)}$	$D_{(free)}$	$D_{(hindered)}$
10/0	2.45×10^{-10}	1.59×10^{-12}	1.54×10^{-10}	8.41×10^{-13}	1.57×10^{-10}	4.17×10^{-13}	2.88×10^{-11}	2.70×10^{-13}
8/2	4.40×10^{-11}	8.44×10^{-13}	2.27×10^{-11}	4.41×10^{-13}	1.10×10^{-11}	2.69×10^{-13}	5.57×10^{-12}	1.51×10^{-13}
6/4	4.63×10^{-11}	1.07×10^{-12}	2.35×10^{-11}	5.47×10^{-13}	1.14×10^{-11}	3.06×10^{-13}	5.77×10^{-12}	1.82×10^{-13}
4/6	4.62×10^{-11}	1.07×10^{-12}	2.38×10^{-11}	5.63×10^{-13}	1.11×10^{-11}	3.15×10^{-13}	5.61×10^{-12}	1.64×10^{-13}
2/8	1.04×10^{-10}	1.40×10^{-12}	5.05×10^{-11}	1.29×10^{-12}	2.45×10^{-11}	1.11×10^{-12}	1.60×10^{-11}	6.14×10^{-13}

[a]The values $D_{(free)}$ refer to the free bulk fraction and are derived from the initial steep slope (first four data points) of the decay plots. The values $D_{(hindered)}$ refer to the encapsulated fraction and are determined from the last four data points of the shallow parts of the plots.

allows for a detailed analysis of complex mesoscopic structures. Separate relaxation measurements (see Supporting Information) have shown that all relaxation times are long in comparison to the corresponding waiting periods in the PFG pulse sequence; therefore, the PFG decay curves are mainly influenced by the self-diffusion behavior of the observed components. In the case of the given system, it can be noted that the state of encapsulation for 1,3-butylene glycol and water in the L_α-phase changes significantly with the relation between 1,3-butylene glycol and glycerol. At a relation of 10/0, the relative contribution of encapsulated molecules is insignificant. This is in accordance with the absence of any birefringence in this state (Figure 1, right), as an encapsulation would require the presence of large-scale bilayers. At relations of 8/2, 6/4, and 4/6, approximately 30% of both components are in the encapsulated state, presumably in multilamellar vesicles as shown by the cryo-TEM micrograph in Figure 2. The vesicle walls are likely to cause the birefringence which is observed in this range (Figure 1). These volumes are in the submicrometer regime, as can be deduced from the relatively small dependence of the slopes on the diffusion time. On the subsecond time scale, the borders of the diffusion compartments are impermeable for the 1,3-butylene glycol but easily permeated by water molecules. With a half-life time of 300 ms of water in the encapsulated state, the permeability of the membranes for water may be comparable to the one of a block-copolymer with an extended hydrophobic region[26] but much smaller than, e.g., that for siloxane surfactant membranes.[16]

At highest glycerol contents (2/8 and 0/10), the compartments become highly permeable for both observed molecules, and the relative contribution of the encapsulated volume is reduced to 10% and 2.5%, respectively. The echo decay plots indicate that the diffusion compartments also have enlarged into sizes of several micrometers, as typical dependencies of the slope on Δ together with characteristic oscillations with the gradient strength are detected. The transition into this final state seems to be accompanied by a disappearance of the normal birefringence for the relation 2/8, while shear birefringence is still present

dx.doi.org/10.1021/jp3046565 | J. Phys. Chem. B 2012, 116, 11459−11465

(Figure 1). Surprisingly, normal birefringence as well as shear birefringence is observed for the relation 0/10, even though the volume contribution of the encapsulated phase is reduced to only 2.5% in this state. This may be explained by a very high degree of permeability of the vesicle membranes under this condition. From the spread of the decay curves in Figure 6 b, one can estimate that the average residence time of water molecules in the encapsulated phase is smaller than 50 ms. This changes dramatically if the system is brought into the gel phase. In that state, no indications for a molecular exchange through the vesicle barriers are observed in the decay plot (Figure 6 a). At least within the given observation period of 400 ms, the decay plots are identical within the experimental error range. Hence, the average residence time in the encapsulated state is likely to be larger than 1 s. This is in accordance with the model of bilayer membranes with minimal mobility. Otherwise, the structure remains the same as indicated by an unchanged relative contribution of the encapsulated volume.

CONCLUSIONS

On the basis of PFG-NMR measurements, two different solvent fractions can be distinguished in MLV phases of PC molecules in glycerol–butylene glycol mixtures. The larger fraction of the solvent molecules diffuses freely like in the bulk solvent without the PC molecules. The smaller fraction of the molecules (between 2.5 and 30%, depending on the solvent composition) is strongly hindered in its mobility. This fraction can be related to the molecules inside the vesicles. On cooling the samples to temperatures below the melting point of the PC, the phases gellify. The gelation is due to the transformation of PC bilayers from the liquid crystalline state into the crystalline state. The volume fraction of the entrapped solvent molecules remains the same over the gelation process. It is assumed that the gelation process is due to the formation of a three-dimensional network of the vesicles. With the PC molecules of the bilayers in the crystalline state, the bilayers can no longer undergo undulations, and the vesicles can now form sticky contacts.

The permeability of the bilayers for small molecules decreases dramatically during the gelation process. Hereby, the average residence time in the encapsulated state increases from less than 50 ms to more than 1 s for water molecules. It is assumed that the crystalline vesicles can be used for the entrapment of drugs and for slow drug release in pharmaceutical formulations. It is conceivable that the permeability of the bilayers in the liquid crystalline and in the crystalline state can be optimized to a desired rate for the release of the drug.

While the crystalline vesicles in the glycerol-containing solvent mixtures were the crucial structures for the gelation of the samples, the gelation in the pure butylene glycol solutions has a different mechanism. PC molecules in pure butylene glycol do not form vesicles. However, on cooling the solutions below T_m, the phases also transform into gels. All the solvent molecules can diffuse freely in these gels. It is therefore assumed that this gel state is due to the formation of a three-dimensional network from crystalline fibers. The network does not entrap solvent molecules.

ASSOCIATED CONTENT

Supporting Information

Spin–spin and spin–lattice relaxation profiles; average residence time in the encapsulated state. This material is available free of charge via the Internet at http://pubs.acs.org.

AUTHOR INFORMATION

Corresponding Author

*E-mail christian.mayer@uni-due.de, tel. +49 (0201) 183-2570, fax +49 (0201) 183-2567.

Notes

The authors declare no competing financial interest.

REFERENCES

(1) Ninham, B. W.; Evans, D. F.; Wei, G. J. *J. Phys. Chem.* **1983**, *87*, 5020.
(2) Larsson, K. *J. Dispersion Sci. Technol.* **1989**, *10* (4, 5), 351–362.
(3) Seddon, J. M. *Biochim. Biophys. Acta* **1990**, *1031*, 1–69.
(4) Boden, N.; Sixl, F. *Faraday Discuss. Chem. Soc.* **1986**, *81*, 191–199.
(5) Sadaghiani, A. S.; Khan, A.; Lindman, B. *J. Colloid Interface Sci.* **1989**, *132* (2), 352–362.
(6) Leneveu, D. M.; Rand, R. P. *Biophys. J.* **1977**, *18*, 209–230.
(7) Brady, J. E.; Fennell Evans, D.; Kachar, B.; Ninham, B. W. *J. Am. Chem. Soc.* **1984**, *106*, 4279.
(8) Jousma, H.; Talsma, H.; Spies, F.; Joosten, J. G. H.; Junginger, H. E.; Crommelin, D. J. A. *Int. J. Pharm.* **1987**, *35*, 263–274.
(9) Aarts, P. A. M. M.; Gijzeman, O. L. J.; Kremer, J. M. H.; Wiersema, P. H. *Chem. Phys. Lipids* **1977**, *19*, 267–274.
(10) Song, A.; Reizlein, K.; Hoffmann, H. *Prog. Colloid Polym. Sci.* **2008**, *134*, 111–119.
(11) Yun, Y.; Hoffman, H.; Richter, W.; Talmon, I.; Makarsky, E. *J. Phys. Chem. B* **2007**, *111*, 6374–6382.
(12) Shinto, K.; Hoffmann, H.; Watanabe, K.; Teshigawara, T. *Colloid Polym. Sci.* **2012**, *290*, 91–95.
(13) Lipowsky, R. *Nature* **1991**, *349* (6309), 475–481.
(14) Gröger, S.; Rittig, F.; Stallmach, F.; Almdal, K.; Stepanek, P.; Papadakis, C. M. *J. Chem. Phys.* **2002**, *117* (1), 396–406.
(15) Nyden, M.; Södermann, O. *Langmuir* **1995**, *11*, 1537.
(16) Yan, Y.; Hoffmann, H.; Leson, A.; Mayer, C. *J. Phys. Chem. B* **2007**, *110* (22), 6161–6166.
(17) Rahem, R. A.; Hoffmann, H. 2012, manuscript in preparation
(18) Hoffmann, H. *Bunsen-Ges. Phys. Chem.* **1994**, *98*, 1433–1455.
(19) Talmon, I.; Hoffmann, H. 2012, manuscript in preparation.
(20) Balinov, B.; Jönsson, B.; Linse, P.; Södermann, O. *J. Magn. Reson. A* **1993**, *104*, 17–25.
(21) (a) Callaghan, P. T. *J. Magn. Reson.* **1995**, *113*, 53–59. (b) Codd, S. L.; Callaghan, P. T. *J. Magn. Reson.* **1999**, *137*, 358–372.
(22) Stejskal, E. O.; Tanner, J. E. *J. Chem. Phys.* **1965**, *42*, 288.
(23) Stejskal, E. O. *J. Chem. Phys.* **1965**, *43*, 3597.
(24) Tanner, J. E.; Stejskal, E. O. *J. Chem. Phys.* **1968**, *49*, 1768.
(25) Kimmich, R. *NMR Tomography, Diffusometry, Relaxometry*; Springer: Berlin, Germany, 1997.
(26) Leson, A.; Filiz, V.; Förster, S.; Mayer, C. *Chem. Phys. Lett.* **2007**, *444*, 268–272.